Electronic Supplementary Information

Fixing of high soluble Br_2/Br^- in porous carbon as cathode material for rechargeable lithium ion batteries

Y.L. Wang, X. Wang, L. Y. Tian, Y. Y. Sun, and S. H. Ye*

Solubility of LiBr in the Electrolytes

The saturated concentration of LiBr in the electrolyte is determined (66.2 g L^{-1}, 0.828 mol L^{-1}) using ion chromatography. The electrolyte is lithium bis(trifluoromethane)sulfonimide (LiTFSI) (1 M) and anhydrous lithium nitrate (0.2 M) dissolved in a mixture of 1,3-dioxolane (DOL) and tetra ethylene glycol dimethyl ether (TEGDME) with a volume ratio of 1:1. The ether-based electrolyte is generally used to Li-sulfur batteries. [1, 2] The saturated LiBr in the electrolyte solution (2 ml) is diluted to 1/25, then 1/100 with water. The diluted LiBr aqueous solution is injected to SH-AC-1C anion exchange column (Dx-120 ion chromatography, DIONEX, US). The mobile phase is Na_2CO_3 (3.5 mmol L^{-1}) and $NaHCO_3$ (1 mmol L^{-1}) aqueous solution. The flow rate is 1.0 mL min^{-1}. Another commercial carbonate-based electrolyte, composed of 1M $LiPF_6$ in ethyl carbonate (EC)/dimethyl carbonate (DMC)/ethyl-methyl carbonate (EMC) with the volumetric ratio of 1:1:1, is also determined for the saturated concentration of LiBr. The saturated concentration is 93.3 g L^{-1} (1.074 mol L^{-1}) at 17°C via a silver ion titration method. In the carbonate-based electrolyte, the as-prepared LiBr-CCB composites exhibit a low initial coulombic efficiency and bad cyclic capacity. Therefore, the ether-base electrolyte above mentioned is selected as the optimal electrolyte for the electrochemical performance of LiBr-CCB composites.

The LiBr content of the as-prepared LiBr/CCB composite is about 0.4 mg (the classical weight of cathode electrode is about 2.0 mg). Six drops of electrolyte are added in the Li/LiBr-CCB batteries (0.126 ml, 2.1 ml/100 drops). Thus, the LiBr concentrate can be calculated as 0.0364 mol L^{-1}. If without the fixing affection of nanopores of CCB substrate, the LiBr in the composite is completely capable of dissolving in the electrolytes above mentioned.

Experimental details

The as-prepared composite was characterized by X-ray diffraction (XRD, Rigaku MiniFlex Ⅱ), thermo-gravimetry analysis (Mettler Toledo, TGA/DSC), Brunauer-Emmett-Taylor (BET, JW-BK), scanning election microscopy (SEM, Hitachi S-4800) and transmission election microscopy (TEM, FEI Tecnai F20).

The working electrode was prepared by compressing a mixture of the LiBr-CCB composite, acetylene black, and the binder poly-tetrafluoroethylene (PTFE) in a weight ratio of 70:20:10 with ethanol as dispersant. Lithium metal was used as the counter and reference electrodes, and a microporous polypropylene film (Celgard 2300) was used as a separator. The electrolyte was LiTFSI (1 M) and anhydrous lithium nitrate (0.2 M, analytical grade) dissolved in a mixture of 1,3-dioxolane (DOL) and tetra ethylene glycol dimethyl ether (TEGDME) with a volume ratio of 1:1.

X-ray Diffraction (XRD)

XRD patterns of the LiBr (3.464 g cm^{-3}), conductive carbon black (CCB, 0.110 g cm^{-3}) and the LiBr-CCB composite are presented in Fig. S1 a. As comparisons, the commercial LiBr and CCB with the weight ratio of 3:7 are mixed in an agate mortar, as shown in Fig. S1 b. The LiBr phase cannot be observed in the XRD spectra both of the LiBr-CCB composite and the mixture, which should be due to the very low volume percentage of LiBr in the composites (1.28%) and the mixture (1.34%).

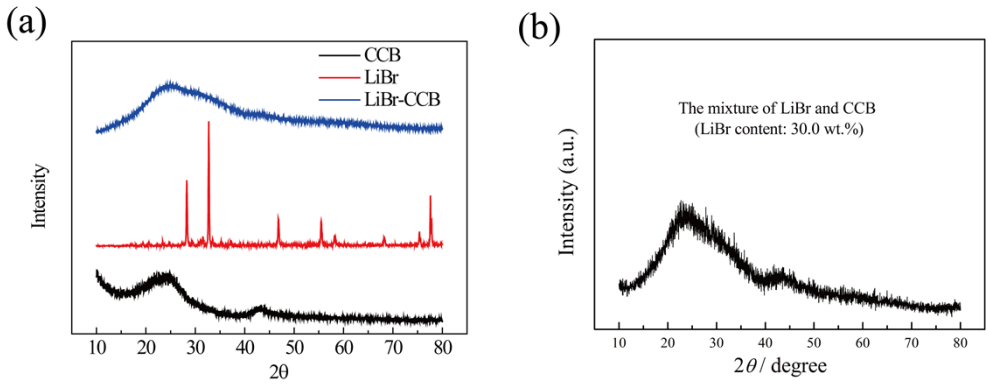

Fig. S1. XRD spectra of a) LiBr, CCB substrate and LiBr-CCB composite; b) the mixture of comercial LiBr and CCB (LiBr content: 30.0 wt.%).

Content of LiBr in Composites

To determine the content of LiBr in the composite, thermogravimetry (TG) was used to test the LiBr-CCB composite within the temperature range of 30-800°C under air atmosphere. Fig. S2 shows the TG curve of the LiBr-CCB composite. There is a small loss under the temperature of 200°C, due to the loss of crystal water in $LiBr{\cdot}3H_2O$. At the temperature of 400-450°C, the curve shows a sharp weight loss corresponding to the oxidation of carbon. The fusion of LiBr in air gives rise to the weight loss above 500°C and it is completely evaporated above 700°C. The accurate content of LiBr in the heat-treated LiBr-CCB composite is 29.01%.

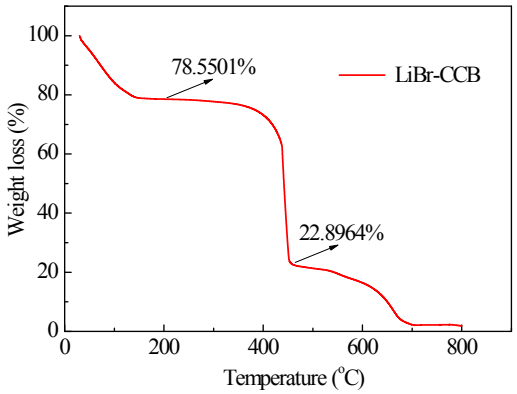

Fig. S2. TG curve of LiBr-CCB composite in air atmosphere

Pore Structure Analysis of CCB and Composites

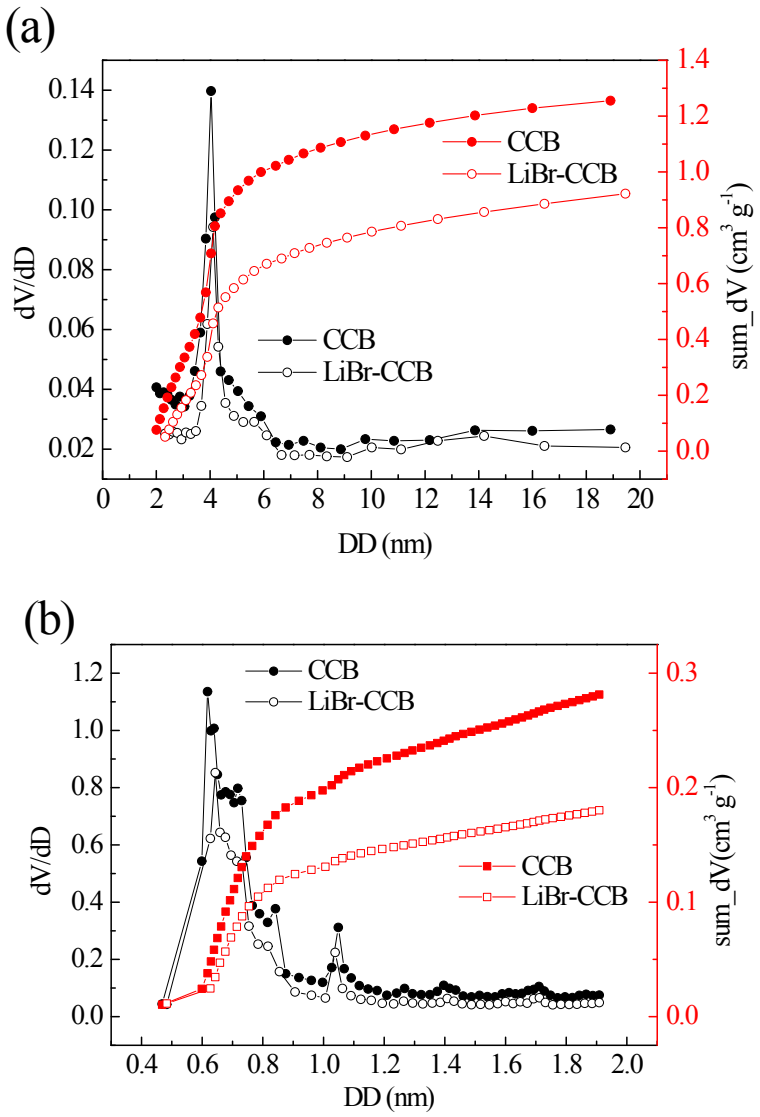

Fig. S3. a) BJH mesopores distributions and b) HK micropores distributions of blank CCB substrate and as-prepared LiBr-CCB composite.

Table S1. The specific surface area and pore volume of CCB and LiBr-CCB composite

Sample	S_{BJH}[a)] [$m^2\ g^{-1}$]	S_{HK}[b)] [$m^2\ g^{-1}$]	V_{meso}[c)] [$m^3\ g^{-1}$]	V_{micro}[d)] [$m^3\ g^{-1}$]	D_{meso}[e)] [nm]	D_{micro}[f)] [nm]
CCB	1081.8	664.9	1.26	0.28	4.03	0.61
LiBr-CCB	693.7	442.2	0.87	0.18	4.18	0.65

[a)]BJH desorption cumulative surface area of pores between 2-300 nm; [b)]Micropore surface area of pores between 0-2 nm; [c)]BJH adsorption cumulative volume of mesopores; [d)]HK adsorption cumulative volume of micropores; [e)]BJH most frequent pore diameter; [f)]HK most frequent pore diameter

The BET surface areas, pore size distributions and porous volumes of the conductive carbon black (CCB) and the as-prepared LiBr-CCB composite were obtained from nitrogen adsorption-desorption curves. It is confirmed that the CCB is composed of spherical carbon nanoparticles with a large specific area. Fig. S3 a and b show BJH mesopores distribution and mesopores volume and the HK micropore distributions and micropore volumes of CCB and the LiBr-CCB composite respectively. The detailed results are given in Table 1. For the blank CCB substrate, the BJH adsorption cumulative pore volume between 2-300 nm is 1.26 $cm^3\ g^{-1}$, the most frequent mesopore size is 4.18 nm, and the BET surface area is 1081.8 $m^2\ g^{-1}$. The HK adsorption cumulative pore volume between 0-2 nm is 0.28 $cm^3\ g^{-1}$, the most frequent micropore size is 0.61 nm, and the surface area is 664.9 $m^2\ g^{-1}$. In the case of the as-prepared LiBr-CCB composite, the BJH adsorption cumulative pore volume and BET surface area decrease to approximately 0.87 $cm^3\ g^{-1}$ and 693.7 $cm^2\ g^{-1}$. The HK pore volume and surface area decrease to approximately 0.18 $cm^3\ g^{-1}$ and 442.2 $cm^2\ g^{-1}$. The decrease of surface areas and pore volumes is due to the LiBr loading in the nanopores of CCB. In addition, the nanopores of CCB have not been fully filled with LiBr.

Morphology and Microstructure

Scanning electron microscopy (SEM) is employed to analyze the morphology of the CCB substrate and the as-prepared LiBr-CCB composite (Fig. S4). The bright field images of CCB and LiBr-CCB samples show that CCB is composed of spherical carbon nanoparticles, with a diameter of about 20-40 nm, and no obvious change is observed after LiBr is loaded onto CCB. Fig. S4 d shows the energy dispersive X-ray spectroscopy (EDS) of the LiBr-CCB composite, corresponding to the point shown in Fig. S4 c. The presence of the element bromine in the composite is confirmed by the EDS analysis. The content of elemental bromine is about 23.36 wt.%, correspondingly, the content of LiBr is 24.90 wt.%. It is similar to the content of 29.01 wt.% measured by thermogravimetry analysis (TG) (Supplementary Fig. S2).

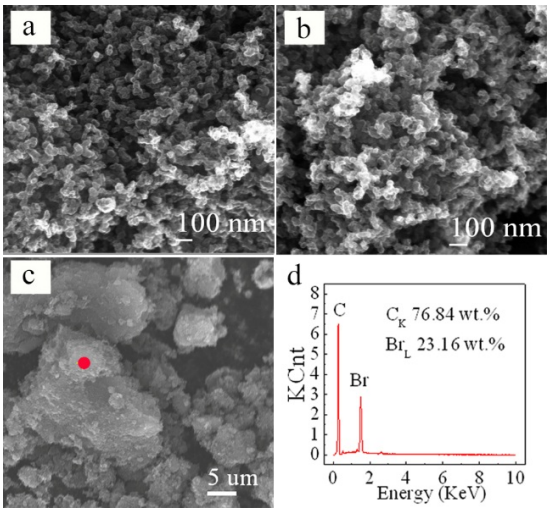

Fig. S4. a) SEM image of the CCB substrate; b, c) SEM images of the as-prepared LiBr-CCB composite; d) the corresponding EDS analysis

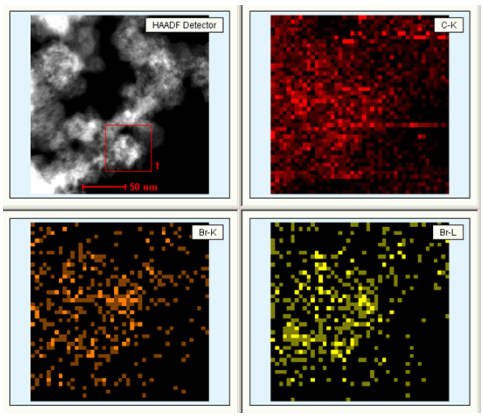

Fig. S5. HAADF-STEM images and the corresponding EDX elemental maps. The elemental map signals are obtained by scanning squre 1 in HAADF-STEM image.

Fig. S5 shows the high-angle annular dark-field scanning transmission electron microscopy (HAADF-STEM) image and the corresponding EDX elemental maps of carbon and bromine. The uniform distribution of carbon and bromine elements implies that the LiBr active mass should be uniformly loaded in the CCB substrate.

Cycle Performance of CCB and the LiBr-CCB Composites

The cycle performance of CCB and the LiBr-CCB composite at the charge-discharge rate (1C) are presented in Fig. S6. In the case of the LiBr-CCB composite, the initial 5 cycles charge capacity loss and low columbic efficiency can be due to the surface adsorption rather than the slight "shuttle effect" in the initial 5 cycles.[3] After that, the LiBr-CCB composite presents a stable electrochemical performance with

columbic efficiency above 98%, and almost no obvious capacity loss is observed in 100 cycles. The obtained initial charge capacity of 333.1 mAh g^{-1}, calculated based on the mass of LiBr in the composite, is higher than the theoretical capacity of LiBr (308 mAh g^{-1}), indicating an extra capacity contribution of pure CCB substrate during the charge-discharge process. Especially, in the initial charge process, an extra 51.7 mAh g^{-1} capacity should be attributed to the capacitive charge of CCB at 2.6-3.0 V. In order to ascertain the extra capacity contribution of CCB, the non-active mass (including CCB, PTFE and acetylene black according to the weight ratio same as those in the composite electrode) is tested at the same current density, it shows a stable charge-discharge capacity of about 17 mAh g^{-1}. It means the non-active mass (except for LiBr) in this composite delivers the cyclic capacity of 66.7 mAh g^{-1} (17 mAh g^{-1}*79.7/20.3) between the potential region of 3.0 -3.8 V. The charge capacity in the initial cycle devoted by only LiBr is about 214.7 mAh g^{-1}. After the first cycle, the charge and discharge capacities are gradually stable at about 250 mAh g^{-1} and after 100 cycles the capacities remain at about 225 mAh g^{-1}. The discharge capacity retention was over 89.5%.

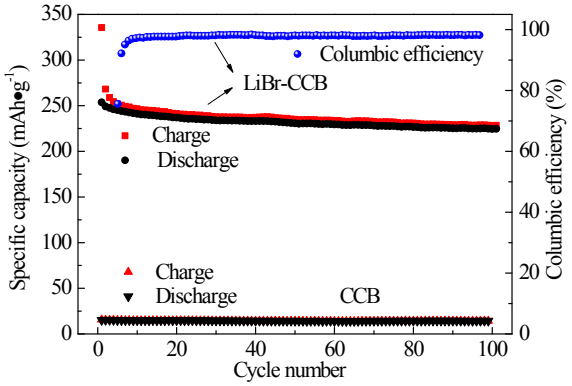

Fig. S6. Cycle performance and columbic efficiency of LiBr-CCB/Li cell at charge-discharge rate of 1C with the cycle performance of pure CCB at the same current density, the materials used in pure CCB is prepared by mixing the CCB, acetylene-black and poly (tetrafluoroethylene) with the weight ratio of 49.7:20:10

Self-discharge Performance

Self-discharge performance is investigated after initial 5 cycles at 1C, shown in Fig. S7. The detailed charge/discharge curves before and after rest for 7 days are shown in Fig. S8. After resting for 7 days, the Li/LiBr-CCB battery still exhibits good discharge capacity and cycleability. During the rest time, the open circuit potential is decreased to 3.4V. After 7 days rest, the recharge capacity is 117.8 mAh g^{-1} at voltage range of 3.4-3.8V, in which a short charge voltage plateau can be observed. That is, some Br_3^- ions are

chemically reduced to Br^- ions during the 7 days. The followed charge capacity at 3.4-3.8V is 175.8 mAh g^{-1}. The difference value is 175.8-117.8=58 mAh g^{-1}, corresponding to amount of Br_3^- ions not chemically reduced during the rest for 7 days. In the following discharge process, the discharge capacity restores to 216.4 mAh g^{-1}. Compared to the discharge capacity before rest, the capacity loss is about 39.1 mAh g^{-1}. Therefore, during the rest for 7 days, all the Br_3^- ions fixed in the nanopores of CCB substrate are partly chemically reduced to Br^- ions, partly still fixed in the nanopores of CCB and partly diffused into the bulk of electrolyte. The cyclic capacity that follows restores to about 216.4 mAh g^{-1} and fades very slowly.

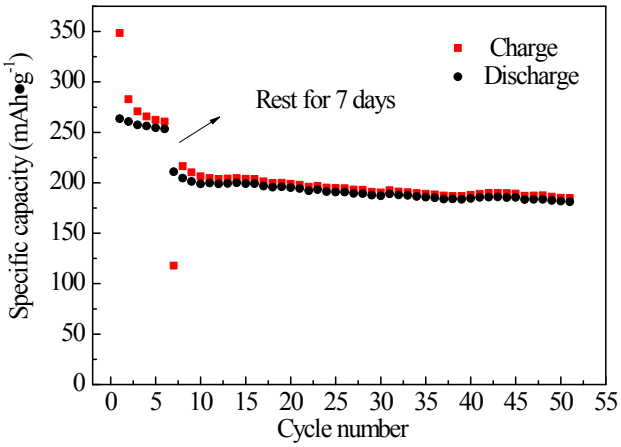

Fig. S7. Self-discharge performance of the LiBr-CCB composites. After 5 cycles at 1C rate, the battery rests for 7 days followed by 45 cycles at 1C rate.

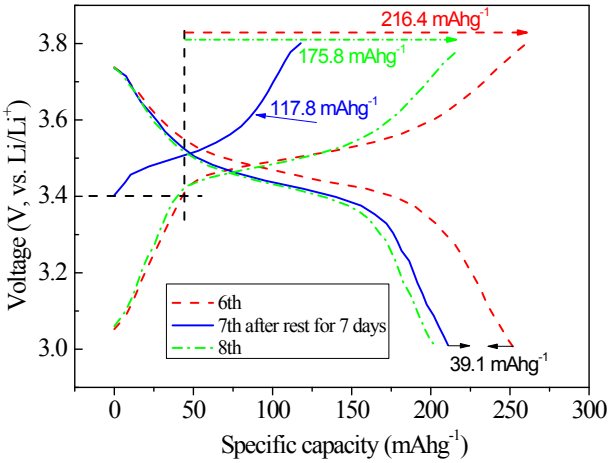

Fig. S8. Charge/discharge curves of the LiBr-CCB composites at 1 C rate before or after resting for 7 days.

Determination of the Li^+ diffusion coefficient by the EIS method

To determined the diffusion coefficient of Li^+ in LiBr-CCB composites, EIS measurement is carried out with an IM6E electrochemical station. The frequency region is from 100 kHz to 0.1 mHz. Fig. S9 shows the Nyquist plots of the Li/LiBr-CCB cell at the initial open circuit potential (3.4 V), 1st full charged state

(3.8 V) and the 2nd full discharge state (2.0 V). The equivalent circuit is inserted in Fig. S9. The Nyquist plots present a typical Nyquist of porous carbon plus a charge transfer process.[4] All three plots are composed of a semi-circle at a middle-high frequency region, a line at a low frequency region. Sequentially, they are related to a charge tranfer impedance, *R*ct and a semi-infinite diffusion, *W*o, respectively.[5] The fitting data are listed in Table S2, which exibit a similar contact resistance and CPE. The charge transfer impedance and Warburg impedance is decreased with cycles. It is noted that the Warburg impedance is about half of the charge transfer impedance. It means the diffusion of Li^+ in the whole reaction is very rapid.

Because of the apparent self-discharged of the composites, the conventional potentiostatic intermittent titration technique (PITT) is not appropriate for the determination of diffusion coefficient of Li^+. The modified EIS method is applied to determined it according the equation $\psi = \sqrt{(\omega L^2)/(2D)}$.[5] ψ is determined the slope of $[d(Z_{Im})/d(Z_{Re})]$ in the diffusion-controlled region.[5] Thus, with angular frequency ω and the distance of diffusion *R* known, the diffusion coefficient of Li^+ is obtained. *R* value is the half of thickness of electrode (0.01 cm). Thus, the average *D* value is calculated as $1.87*10^{-5}$ cm^2 S^{-1}. It is one order of magnitude smaller than the diffusion coefficient of proton in bulk water ($1.2*10^{-4}$ cm^2 S^{-1}).[6] Combined the fitting data listed in Table S1, compared with *R*ct value the smaller Warburg impedance implies the diffusion process is very fast, which is distinct from the solid-phase diffusion reaction.

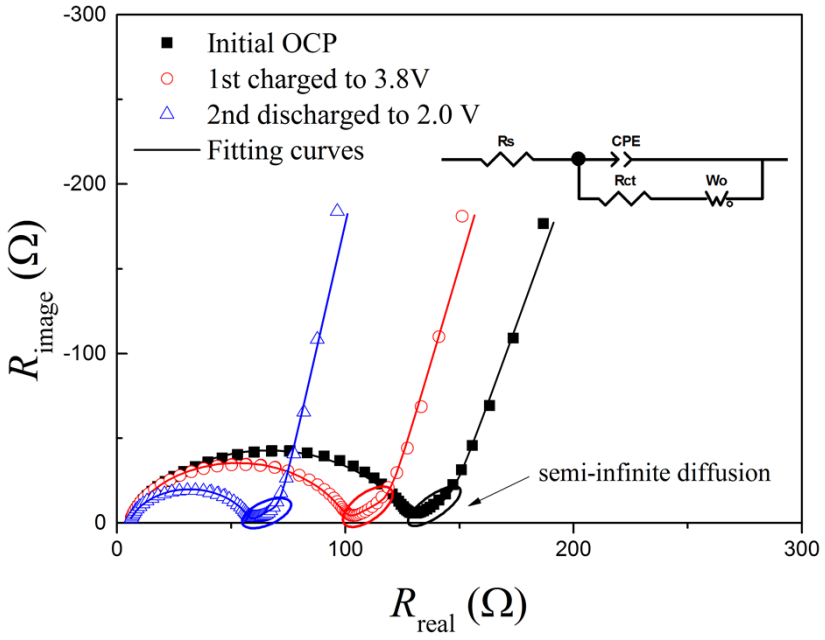

Fig. S9 Nyquist plots of LiBr-CCB composites in LIBs at various potentials (initial OCP, initial charged to 3.8 V and first discharged to 2.0 V). The lines represent the fitting curves. The corrsponding equivalent circuit is serted.

Table S2. EIS equivalent circuit fitting results of Li/LiBr cell at various potential

state of charge	*R*s (Ω)	*CPE* (μF)	*R*ct (Ω)	W_o (Ω)
Initial OCP	5.131	6.7572	121.3	53.07
Initial charged to 3.8 V	4.941	4.929	94.86	52.17
1st discharged to 2.0 V	5.178	5.702	52.81	36.39

*R*s: contact resistance, *CPE*: constant-phase element, *Rct*: charge-transfer impedance, W_o: Warburg impedance

1. W. G. Wang, X. Wang, L. Y. Tian, Y. L. Wang and S. H. Ye, *J. Mater. Chem. A*, 2014, **2**, 4316.
2. T. Yim, M.-S. Park, J.-S. Yu, K. J. Kim, K. Y. Im, J.-H. Kim, G. Jeong, Y. N. Jo, S.-G. Woo, K. S. Kang, I. Lee and Y.-J. Kim, *Electrochim. Acta*, 2013, **107**, 454-460.
3. A. Kaya and A. Schumpe, *Chem. Eng. Sci.*, 2005, **60**, 6504-6510.
4. C. Yang, C.-Y. Vanessa Li, F. Li and K.-Y. Chan, *J. Electrochem. Soc.*, 2013, **160**, H271-H278.
5. P. Yu, B. N. Popov, J. A. Ritter and R. E. White, *J. Electrochem. Soc.*, 1999, **146**, 8-14.
6. M. Gutman, E. Nachliel and S. Moshiach, *Biochemistry*, 1989, **28**, 2936-2940.